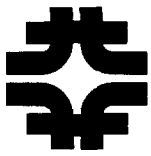

Fermilab

TM-1090

1183.00

Jan. 1982

The Effect of Missing Backscatter on the Dose Distribution of a p(66)Be(49) Neutron Therapy Beam.

I. Rosenberg, M. Awschalom, R. K. Ten Haken

Fermilab Neutron Therapy Facility, P. O. Box 500, Batavia, IL

Abstract.

The dose reduction in phantom due to missing backscattering material was measured on and off the central axis of a p(66)Be(49) neutron beam. The doses at different depths in phantom for various field sizes are found to drop by 4-10% relative to full backscatter conditions when backscattering material is removed. A simple algorithm that predicts the magnitude of this drop on the basis of equivalent square size of the beam is presented. The algorithm may be used to correct the dose (usually computed from data obtained with full backscatter) at all points near the exit side of a phantom or patient.

Key Words: neutrons, p(66)Be(49), backscatter, central axis depth dose.

Introduction.

Patient dose calculations are generally based on data obtained from dose distribution measurements taken in a large homogeneous liquid phantom. However, several differences exist between the idealized conditions under which such discrete measurements are made and the actual environment in which one wishes to predict continuous dose distributions. These differences include: (a) dose attenuation and scatter of the therapy beam may not be the same in the phantom material as in human tissues, (b) the human body is not homogeneous, (c) clinical situations might involve oblique incidence of beams and/or curved entrance surfaces, and (d) patients' cross sections may be considerably smaller than those of the measurement phantom. Therefore, in addition to assessing the accuracy of the method used to store, reproduce, and interpolate between measured dose distributions, one must look into the sources of error introduced by the above physical differences. The problems mentioned affect both photon and neutron beams, but their importance varies with the microscopic processes involved. They should, therefore, be assessed anew for each different quality beam. In what follows, we concentrate on how tissue missing at the beam exit side of a patient affects the dose distribution of a particular neutron therapy beam.

It has long been known that lack of backscattering material will affect the photon dose at the exit side of a phantom[1-4], and a recent study showed that these effects can be noticed in the material well upstream of the exit surface.[5] Similar effects are found in low penetration neutron therapy beams.[6,7] This report presents results obtained with the most penetrating neutron therapy beam currently in use in the U. S. A.

Experimental Methods.

The p(66)Be(49) fast neutron beam at Fermilab[8,9] was used for this experiment. Its physical characteristics have been described elsewhere.[10,11]

The detector used was a cylindrical parallel plate ionization chamber, designed and built by Professor J. J. Spokas of Illinois Benedictine College in collaboration with the authors. It is composed almost exclusively of A-150 Tissue Equivalent plastic,[12] for homogeneity, with small teflon screws and thin teflon insulators. A simplified cross-section of this chamber is given in Fig. 1. The thickness of the collector and rear assembly is 9 mm. The connecting cable and gas lines are at the side of the chamber, to minimize the perturbation of the particle flux seen by the collecting volume.

The chamber itself was imbedded coaxially in a 36 cm diameter disk of A-150, such that its outer electrode was recessed about 0.5 mm from one face of the disk and the total amount of A-150 between its collector surface and the other face of the disk was 2.5 cm. The chamber was vented to the atmosphere, and it was operated at +600 V collecting voltage, which ensured adequate saturation. Its output, and the output of the monitor transmission chamber, were processed and continuously corrected for temperature and pressure effects by the microcomputer-based dosimetry system described elsewhere.[13]

This parallel plate chamber was designed specifically to have minimal perturbation effects on radiation fields, to be as homogeneous and symmetrical as possible and thus function properly in the reversed orientation needed for this investigation. To test these design goals, the chamber was sandwiched symmetrically between its own disk and another similar one, such that 2.5 cm were present on both sides of the collecting volume. Irradiating the ensemble through either disk face at constant SSD yielded the same ionization per monitor unit within the 0.3% precision of the measurements.

The experimental set-up is illustrated in Fig. 2. The disk containing the chamber was positioned coaxially with the beam axis, with the outer electrode facing away from the neutron source. The various phantom and backscatter thicknesses were

achieved by placing additional 36 cm diameter A-150 disks coaxially with the chamber upstream and downstream, respectively, of the ionization chamber while keeping the SSD fixed at 142.5 cm. Backscatter disks of less than 4 mm in thickness, however, were limited to 19 cm diameter. Field sizes were varied by the use of polyethylene-concrete collimators.[10,13] The equivalent square at the upstream surface of the stack (ESQ) was used to label the radiation field, regardless of the depth of the chamber.

Results and Discussion.

The neutron energy spectrum at the chamber may vary after traversing different thicknesses of phantom and, therefore, possibly change the amount of backscattered radiation in that region. To study this possible variation, measurements were made using stacks of A-150 (density 1.12 g cm^{-3}) with thicknesses of 3, 15, and 24 g cm^{-2} upstream of the collecting volume and two clinically extreme values of field size, a 6x6 cm^2 square and a 28 cm diameter circle (ESQ = 25 cm). For each situation an increase in ionization was observed as backscatter material was added downstream from the chamber. The results are shown in Fig. 3. All measurements are normalized to the values obtained with full backscatter for each situation (achieved with about 30 g cm^{-2} of backscattering material). The uncertainties in the data points, not shown in the figure for clarity, are on the order of 0.2-0.4%

of the quantity measured. The logarithmic abscissa is expressed in terms of the total thickness of A-150 downstream from the collecting volume, and thus the 56 mg cm^{-2} point corresponds to the outer electrode of the chamber alone. The curves drawn on this figure are least square fits to the data of an expression which will be discussed later in this section. As seen in Fig. 3, the two field sizes exhibit different backscatter effects. For the smaller field size, the reduced ionization with progressively less backscattering material is practically the same for all three upstream stack thicknesses and the relative ionization with just the 0.5 mm outer electrode is still about 0.96 in all cases. By contrast, with the larger field size a much greater drop in ionization is observed as less backscattering material is used, and there appears to be a slight dependence on upstream stack thickness, with reduced relative doses with the 0.5 mm outer electrode alone of 0.895, 0.902 and 0.912 ($\pm$0.003) for the 3, 15 and 24 g cm^{-2} stacks, respectively.

In addition to the above field sizes, the effect of missing backscatter was also measured for field sizes of 5.25 x 15 (ESQ = 7.8), 9 x 9, 12 x 12, 15 x 15, and 18 x 18 cm^2 using the 15 g cm^{-2} thick phantom only. Some of the results are shown in Fig. 4, where, again, the ionization with reduced backscatter, normalized to that with full backscatter for each field size, is plotted against the amount of backscattering material in g cm^{-2}, this time on a linear scale. It is obvious from Fig. 4 that the amount of

reduction in ionization depends on field size. For each field size, the relationship of relative dose to backscattering thickness can be approximated by a saturation-like expression of the form:

$$D(t) = 1-A\ e^{-t/B} \qquad (1)$$

where D(t) is the normalized ionization for backscattering thickness t, and A and B are parameters to be determined. Values of A and B were obtained for each field size and each phantom thickness by least squares fits of Eq. 1 to the data. The curves shown in Fig. 3 were computed from best fit parameters to the individual sets of measurements. As can be seen, use of the above expression provides good fits to the data, within the stated uncertainties, except possibly for thicknesses below 150 mg cm^{-2}, where deviations from the measured values approach 1%.

The trend of the values for A and B obtained from the fits to the set of measurements with the 15 g cm^{-2} thick phantom was investigated and linear correlations with field size were found to exist for both parameters. The following regressions were obtained by least squares fits to the values:

$$A = 0.0165 + 0.0030\ ESQ \qquad (r = .99) \qquad (2)$$

$$B = 2.55 + 0.070\ ESQ \qquad (r = .68),$$

where ESQ is the equivalent square of each field at the upstream surface of the phantom, B is expressed in g cm^{-2}, and r is the correlation coefficient. The curves shown in Fig. 4 were computed using Eq. 1 and the values of A and B computed from Eq. 2. It can be seen that the curves provide a satisfactory representation of the measured values, within stated uncertainties, for the field sizes shown in the figure, even for the rectangular and circular fields. These equations reproduce the data equally well for the other square fields, not shown here for clarity. Deviations from the measurements at thicknesses less than 150 mg cm^{-2} still approach 1%, hardly noticeable on the scale shown in Fig. 4.

One further set of measurements was performed to check the behavior of this effect for points not on the central axis of the beam. The 28 cm diameter circular field was used, with an upstream phantom thickness of 15 g cm^{-2}, but with the stack axis displaced 11 cm from the beam axis, corresponding to the 90% off-axis ratio distance. The resulting relative ionizations with varying backscatter thicknesses were practically indistinguishable from the results obtained on the central axis with the 24 g cm^{-2} thick phantom for the same field size (Fig. 3). In other words, the differences between the off-axis and on-axis effects were at most 1%.

A comparison can be made between the present results obtained for a neutron beam and similar measurements made for two photon beams by Gagnon and Horton.[5] For ^{60}Co radiation, they also found that the amount of missing backscatter exhibits a marked dependence on field size as well as a weak dependence on upstream phantom thickness. For backscatter thicknesses of about 100 mg cm^{-2} they found dose reductions, compared to full backscatter conditions, ranging from about 2% for a 6x6 cm^2 field to about 7% for a 20x20 cm^2 field. These values are comparable to those found here with the neutron beam. By contrast, smaller effects were found with a 25 MV x-ray beam, and there was practically no dependence of the dose reduction on field size or upstream phantom thickness.

The results from both photon beam measurements can also be fitted well by an expression in the form of Equation 1 above. The calculated values of reduced dose as a function of backscatter thickness, obtained by a least-square fit of Equation 1 to the data plotted in Ref. 5, agree within 1% with the measurements for backscatter thicknesses larger than 100 mg cm^{-2}. For ^{60}Co, values of the parameter B in Eq. 1, a measure of the range of propagation of the missing backscatter effect, vary from about 2 to 6 g cm^{-2}, depending on field size, which is comparable to the present neutron results, but are on the order of 0.5 g cm^{-2} for the 25 MV x-ray beam.

Summary and Conclusions.

To summarize, we have shown that, for the neutron beam under study: (a) the reduction in dose due to lack of backscattering material beyond the exit surface of a phantom, relative to that predicted from measurements with full backscatter, can be as large as 4-10% near the exit surface and still persists at the 2-3% level up to 5 cm upstream of that surface; (b) the value of this reduced dose can be predicted within 0.5% along the central axis by use of Eqs. 1 and 2, (1% for points within 2 mm of the exit surface), for a phantom of 15 g cm^{-2} thickness, from knowledge of the equivalent square size of the field at the entrance surface; (c) the correction for the reduced dose is only slightly dependent on actual upstream phantom thickness or off-axis distance and, depending on field size, further errors of at most $\pm$1% in dose are introduced when using the above expressions for 3 to 24 g cm^{-2} thick phantoms irrespective of off-axis distance.

It would, therefore, be appropriate to apply corrections computed using the expressions stated above, as a function of a single parameter (ESQ), to all points inside a patient contour when calculating the dose distribution from one or more fields. For most field sizes and patient dimensions encountered in practice this correction will predict the reduced doses to within 1-2%. In principle, higher precision could be achieved in all

cases by adding a second correction term for points closer than 2 mm from the exit surface and by making parameters A and B functions of upstream phantom thickness, as well as equivalent square of the beam.

Digitized contour information is used in many computerized treatment planning systems to correct for the variation of SSD and overlying tissue with off-axis distance for each beam. This is usually achieved for each field by determining the points where a set of rays from the radiation source intersect the contour. During this search, both the proximal and distal intersection points are found, except for tangential rays. Knowledge of these distal intersection points will enable the program to compute, by interpolation, the distance between every calculation point and the exit surface.

Thus, after the computation of the dose contribution from each field is completed, using any beam calculation method, corrections for missing backscatter can be added by means of one additional multiplication, using the above expressions and the appropriate backscatter thickness, at each calculation point. This modification would be especially relevant for treatment plans involving narrow patient anatomy or in other instances where the tumor is situated close to the exit surface of one of the planned fields.

Acknowledgements.

This work was supported in part by NCI Grant 5PO1CA81081-07.

REFERENCES

1. Quimby, E. H., Marinelli, L. D., Farrow, J. H., Am. J. Roentgenol. 39, 799 (1938).

2. Bailey, N. A., Beyer, N. S., "Exit Dosage for 2 MVp X-Rays", Radiology 70, 395 (1958).

3. Goede, M. R., Anderson, D. W., McCrary, K. L., "Corrections to Megavoltage Depth Dose Values Due to Reduced Backscatter Thickness", Med. Phys. 4, 123 (1977).

4. Legare, J.-M., "Central-Axis Depth Dose Data for Phantoms of 0- to 25 cm Thickness in Roentgen, Cesium -137, and Cobalt -60 Therapy", Radiology 92, 1321 (1969).

5. Gagnon, W. F., Horton, J. L., "Physical Factors Affecting Absorbed Dose to the Skin From Co-60 Gamma Rays and 25 MeV X-rays", Med. Phys. 6, 285 (1979).

6. Catterall, M., Bewley, D. K., "Fast Neutrons in the Treatment of Cancer", London: Academic Press, 1979. Chapter 3.

7. Wooton, P., Weaver, K. and Eenmaa, J., "Treatment Planning for Neutron Radiation Therapy", Int. J. Rad.

Oncol. Biol. Phys. 3, 177 (1977).

8. Cohen, L., Awschalom, M., "The Cancer therapy Facility at the Fermi National Accelerator Laboratory, Batavia, Illinois: A Preliminary Report, Appl. Radiology 5, (#6)51-60 (1976).

9. Awschalom, M., Grumboski, L., Hrejsa, A. F., Lee, G. M., Rosenberg, I., "The Fermilab Cancer Therapy Facility: Status Report After 2.5 Years of Operation", IEEE Trans. Nucl. Sci. NS-26 (3) 3068 (1979).

10. Rosenberg, I., Awschalom, M., "Characterization of a p(66)Be(49) Neutron therapy Beam. I: Central Axis Depth Dose and Off-Axis Ratios", Med. Phys. 8, 99(1981).

11. Awschalom, M., Rosenberg, I., "Characterization of a p(66)Be(49) Neutron Therapy Beam. II. Skin-sparing and Dose Transition Effects", Med. Phys. 8, 105(1981).

12. Smathers, J. B., Otte, V. A., Smith, A. R., Almond, P. R., Attix, F. H., Spokas, J. J., Quam, W. M., Gooodman, L. J., "Composition of A-150 Tissue Equivalent Plastic," Med. Phys. 4, 74(1977).

13. Awschalom, M., Rosenberg, I., "Neutron Beam Calibration and Treatment Planning", Fermilab Technical Memorandum

TM-834 (Dec. 1978), pp 93.

FIGURE CAPTIONS.

Fig. 1 - Highly simplified sketch of parallel plate ionization chamber. All components, except where specified, are made out of A-150 plastic.

OE = outer electrode, 0.5 mm thick.

C = collector, 20 mm diameter.

G = guard.

AG = air gap, 1.0 mm thick.

W1, W2 = gaps between collector and guard, 0.13 mm wide.

SS = teflon support screws (3).

I1, I3 = teflon insulators, 0.13 mm thick.

I2 = teflon insulator, 0.25 mm thick.

Fig. 2 - Sketch showing the relative positions of target, collimator, upstream and downstream A-150 disks. ESQ = side of equivalent square of neutron beam.

Fig. 3 - Dose relative to full backscatter versus thickness of backscattering material, for two field sizes (6x6 cm^2 and 28 diameter circle). Symbols correspond to:
X 3 g cm^{-2}, O 15 g cm^{-2}, and Δ 24 g cm^{-2} upstream phantom thicknesses. Curves represent best fits to the data of the expression discussed in the text.

Fig. 4 - Dose relative to full backscatter versus thickness of

backscattering material for field sizes:

□ 12.5 x 15 cm^2 (ESQ = 7.8), ● 12 x 12 cm^2, ■ 18 x 18 cm^2 and O 28 diameter circle (ESQ = 25). Upstream phantom thickness was 15 g cm^{-2} in all cases. Curves represent parametrized fits using the expressions discussed in the text.

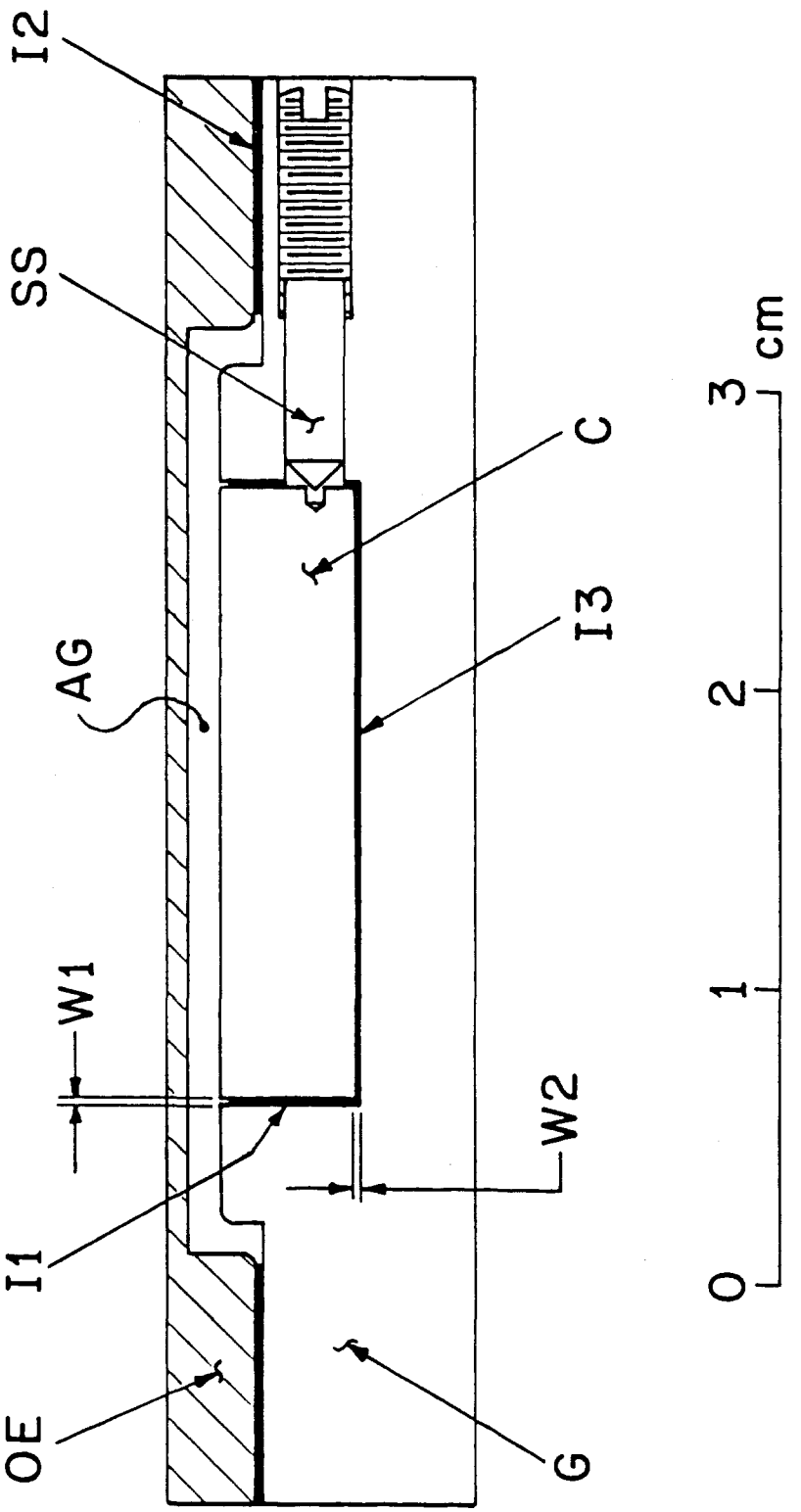

Figure 1

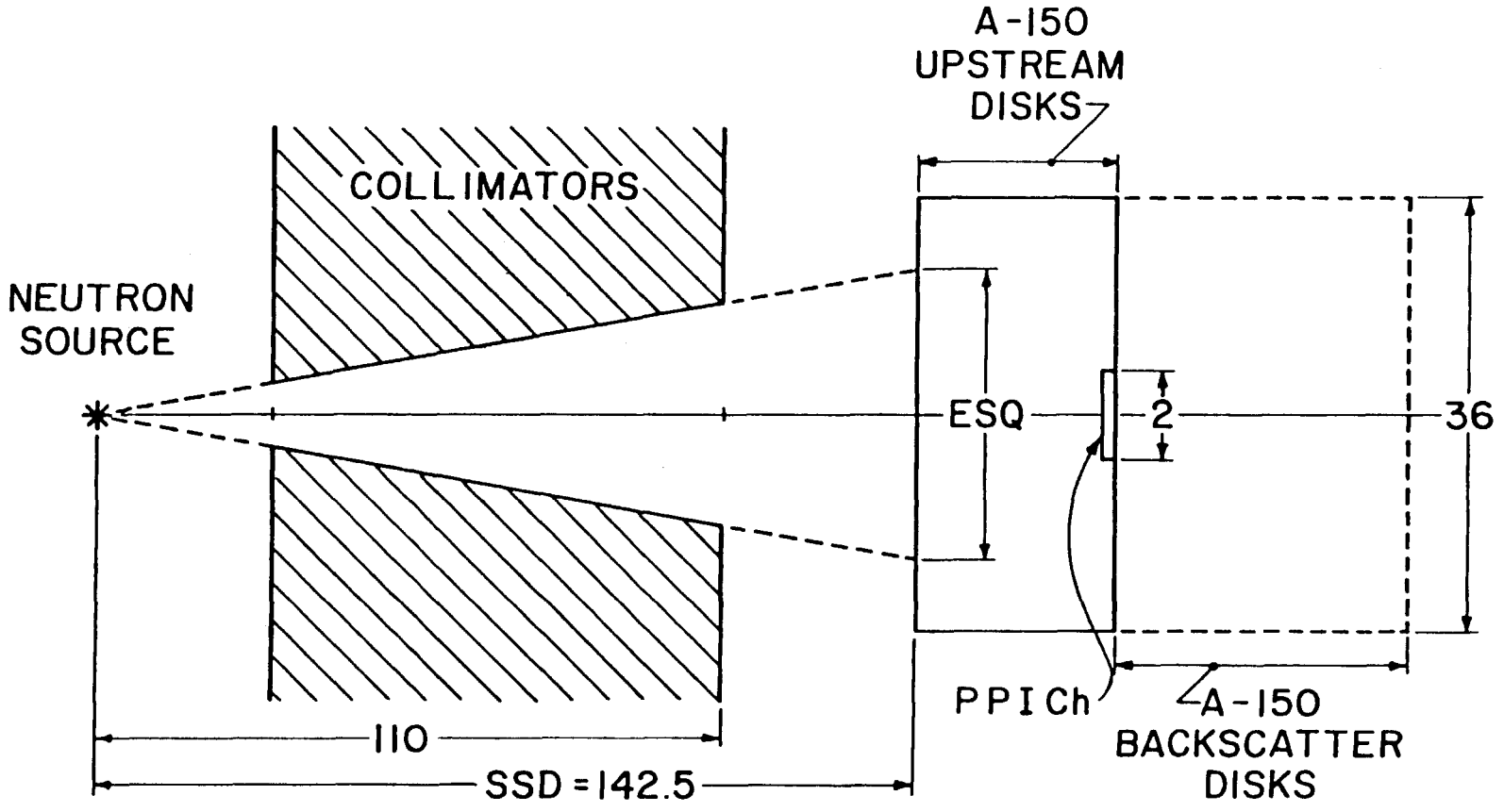

Dimensions in cm

Figure 2

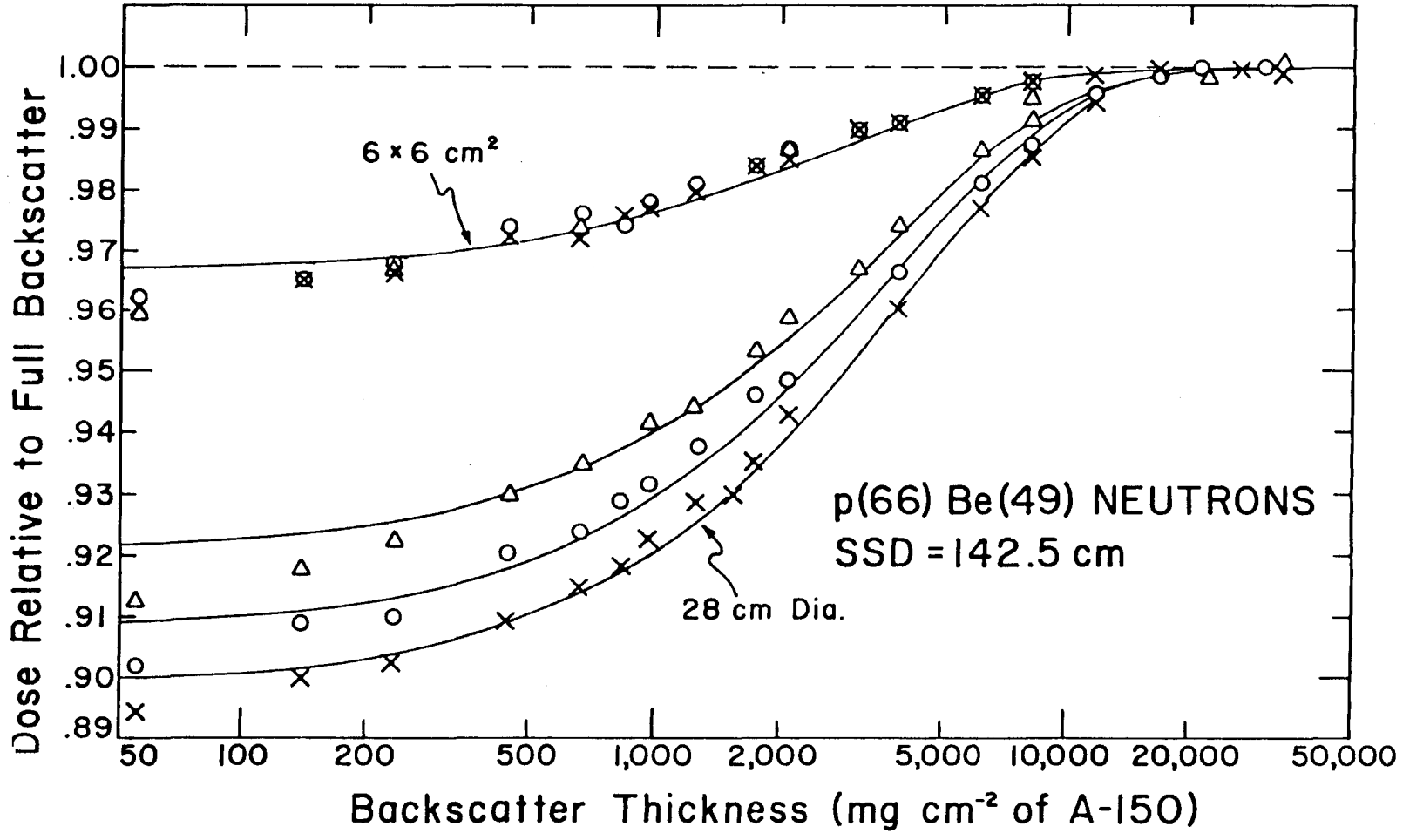
Dose Relative to Full Backscatter
1.00
.99
.98
.97
.96
.95
.94
.93
.92
.91
.90
.89
6 × 6 cm²
p(66) Be(49) NEUTRONS
SSD = 142.5 cm
28 cm Dia.
50
100
200
500
1,000
2,000
5,000
10,000
20,000
50,000
Backscatter Thickness (mg cm⁻² of A-150)

Figure 3

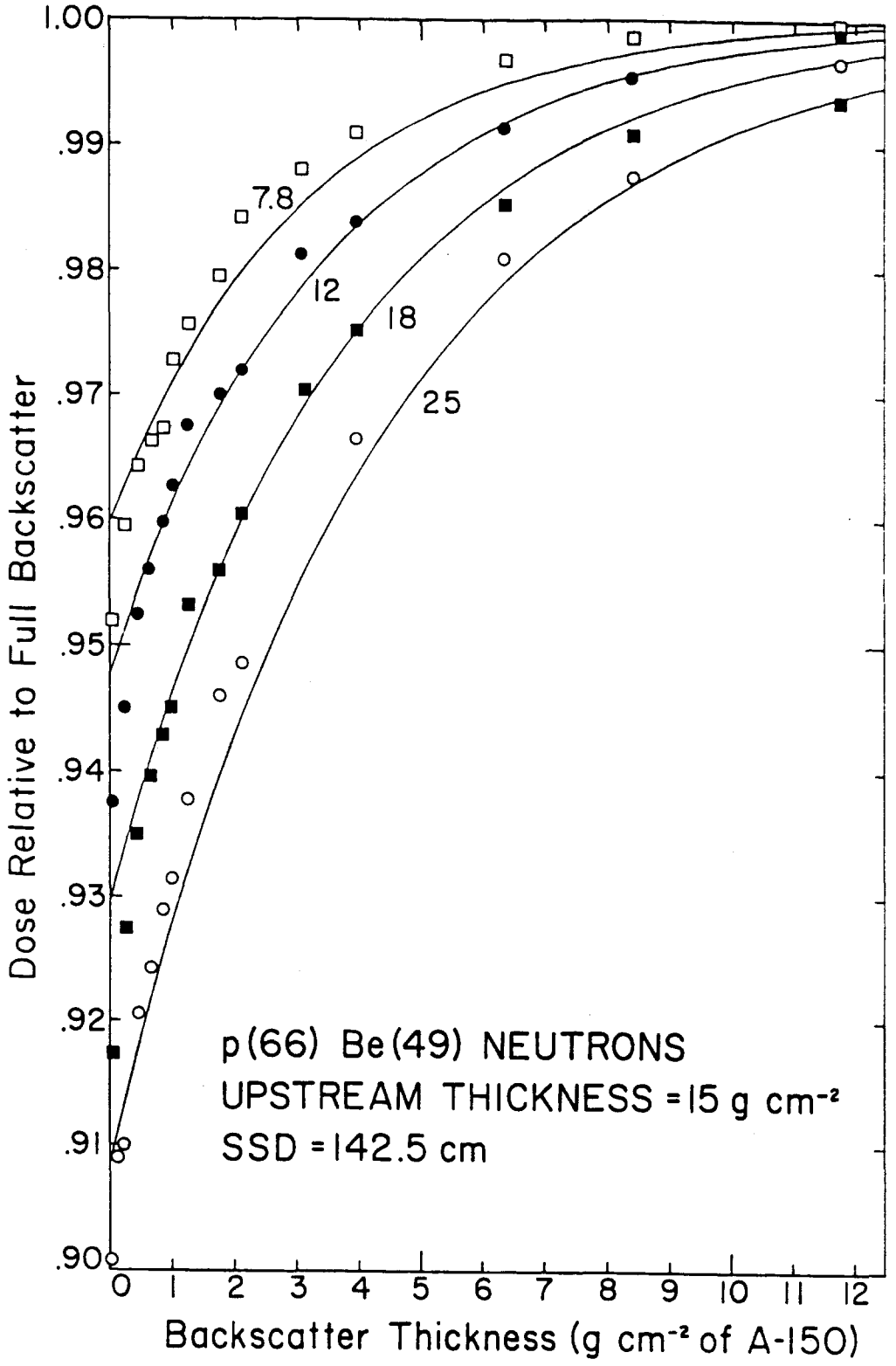
1.00
.99
.98
.97
.96
.95
.94
.93
.92
.91
.90
Dose Relative to Full Backscatter
7.8
12
18
25
p(66) Be(49) NEUTRONS
UPSTREAM THICKNESS = 15 g cm⁻²
SSD = 142.5 cm
0 1 2 3 4 5 6 7 8 9 10 11 12
Backscatter Thickness (g cm⁻² of A-150)

Figure 4